PROF. IRENE O.L. NG (Orcid ID : 0000-0001-7532-2029)
DR. STEPHANIE KWAI YEE MA (Orcid ID : 0000-0002-2029-7943)
DR. TERENCE K LEE (Orcid ID : 0000-0003-0682-322X)

Article type : Original

HEP-19-1016.R1

Overriding adaptive resistance to sorafenib via combination therapy with SHP2 blockade in hepatocellular carcinoma

Carmen Oi Ning Leung [1*], Man Tong [2*], Katherine Po Sin Chung[1], Lena Zhou[2], Noélia Che[2], Kwan Ho Tang[3^], Jin Ding[4], Eunice Yuen Ting Lau[5], Irene Oi Lin Ng[6,7], Stephanie Ma[2,7#], Terence Kin Wah Lee[1,8 #]

[1]Department of Applied Biology and Chemical Technology, The Hong Kong Polytechnic University, [2]School of Biomedical Sciences, Li Ka Shing Faculty of Medicine, The University of Hong Kong, [3]Laura and Isaac Perlmutter Cancer Center, New York University School of Medicine, NYU Langone Health, New York, [4]Eastern Hepatobiliary Surgery Hospital, The International Cooperation Laboratory on Signal Transduction, [5]Department of Clinical Oncology, Queen Elizabeth Hospital, [6]Department of Pathology, The University of Hong Kong, [7]State Key Laboratory for Liver Research, The University of Hong Kong, [8]State Key Laboratory of Chemical Biology and Drug Discovery, The Hong Kong Polytechnic University

*Contributed equally

^ Senior author

[#]Corresponding authors:

[1]The address of Dr. Terence K.W. Lee is Room 805, Block Y, Department of Applied Biology and Chemical Technology, Lee Shau Kee Building, The Hong Kong Polytechnic University, Hong Kong. Tel: (852) 3400-8799; Fax: (852) 2364-9932; Email: terence.kw.lee@polyu.edu.hk. [2]The address of Dr. Stephanie Ma is L1-47, Laboratory Block, School of Biomedical Sciences, The University of Hong Kong, Hong Kong. Tel: (852) 3917-9238; Fax: (852) 2817-0857; Email: stefma@hku.hk.

Running title: Combined SHP2 inhibition with sorafenib in HCC

Keywords: HCC, RTK, SHP2, sorafenib

Abbreviations: cancer stem cells, CSCs; extracellular signal-regulated kinase, ERK; hepatocellular carcinoma, HCC; hydrodynamic transfection, HT; MEK inhibitors, MEKI; mitogen-activated protein kinase, MAPK; phosphoinositide 3-kinase, PI3K; patient derived tumor xenografts, PDTXs; quantitative reverse transcription polymerase reaction, qRT-PCR; receptor tyrosine kinase, RTK; Src homology 2 domain–containing phosphatase 2, SHP2; tyrosine kinase inhibitors, TKIs.

Grant Support: This study was supported by the Research Grants Council of Hong Kong - Collaborative Research Fund (C7026-18G).

Competing financial interests: The authors declare no competing financial interests.

Authors Contributions: C.O.L., M.T., S.M., and T.K. designed the experiment. C.O.L., M.T., K.P.C., Z.L., N.C., E.Y.L. performed the experiment. C.O.L., M.T., K.H.T., S.M., and T.K. analyzed the data, C.O.L., M.T., S.M., and T.K.L. wrote the paper. J.D., and I.O.N. provided reagents, advices and PDTX for this study. T.K.L., and S.M. supervised the study. All authors contributed to the discussion of results and manuscript corrections.

Abstract

The survival benefit of sorafenib for hepatocellular carcinoma (HCC) patients is unsatisfactory due to the development of adaptive resistance. Increasing evidence has demonstrated that drug resistance can be acquired by cancer cells by activating a number of signaling pathways via receptor tyrosine kinases (RTKs), nevertheless the detailed mechanism for the activation of these alternative pathways is not fully understood. Given the physiological role of Src-homology 2 domain–containing phosphatase 2 (SHP2) as a downstream effector of many RTKs for activation various signaling cascades, we first found that SHP2 was markedly upregulated in our established sorafenib-resistant cell lines as well as patient-derived xenograft (PDTX). Upon sorafenib treatment, adaptive resistance was acquired in HCC cells via activation of RTKs including AXL, EGFR, EPHA2 and IGF1R, leading to RAS/MEK/ERK and AKT reactivation. We found that SHP2 inhibitor SHP099 abrogated sorafenib resistance in HCC cell lines and organoid culture *in vitro* by blocking this negative feedback mechanism. Interestingly, this sensitization effect was also mediated by induction of cellular senescence. SHP099 in combination with sorafenib was highly efficacious in the treatment of xenografts and genetically engineered models of HCC. In conclusion, SHP2 blockade by SHP099 in combination with sorafenib attenuated the adaptive resistance to sorafenib by impeding RTK-induced reactivation of the MEK/ERK and AKT signaling pathways. SHP099 in combination with sorafenib may be a novel and safe therapeutic strategy against HCC.

Introduction

Liver cancer (hepatocellular carcinoma, HCC) is one of the deadliest diseases, being the 6th most commonly diagnosed cancer and the 4th leading cause of cancer mortality in the world.(1) HCC treatment recently entered a new era with the development of molecular-targeted therapies, and sorafenib has resulted in improvement in the survival of advanced HCC patients.(2) Sorafenib, a multikinase inhibitor, blocks tumor cell proliferation by specifically targeting multiple growth factor pathways, and it exerts an anti-angiogenic effect. Two large-scale phase 3 randomized clinical trials, including the SHARP trial,(3) have demonstrated a survival benefit in advanced HCC patients.(4) However, the survival benefit in the sorafenib treatment arm was modest; the median survival was only 2.8 and 2.3 months longer than that of the placebo arm in the two large-scale trials in Caucasians and Asians, respectively.(3,4) This unsatisfactory partial response may be due to drug resistance.(4,5) To prolong the survival of HCC patients, combination therapy targeting multiple signaling pathways may serve as a better treatment option by potentially circumventing drug resistance.

Increasing evidence has demonstrated that drug resistance can be acquired by cancer cells by activating a modified signaling pathway through receptor tyrosine kinases (RTKs) to replace the loss of signal in response to various tyrosine kinase inhibitors (TKIs). For instance, EGFR mutant lung cancer cells can acquire resistance to EGFR-TKIs via HGF/MET-mediated activation of mitogen activated protein kinase (MAPK)/extracellular signal regulated kinase (ERK)1/2 and phosphoinositide 3-kinase (PI3K)/AKT signaling.(6) Additionally, activation of IGFR-1β via upregulation of insulin-like growth factor II expression can compensate for the loss of EGFR signaling caused by gefitinib in colorectal cancer.(7) Specifically, in HCC, activation of PI3K/AKT signaling(8) and ERK(9) in HCC was found in HCC cells in response to sorafenib; however, the detailed mechanism for the activation of these alternative pathways is not fully understood. Therefore, it is critical to identify the RTK reactivation-mediated mechanism of adaptive resistance of HCC cells in response to sorafenib treatment. In previous studies, we found that Src-homology 2 domain–containing phosphatase 2 (SHP2), encoded by PTPN11, was not only overexpressed in HCC(10) but could also serve as a predictive biomarker for sorafenib response and patient survival.(10) This, together with data showing a sensitization effect to sorafenib upon SHP2 suppression,(11) suggests a potential therapeutic strategy

against HCC by targeting SHP2 expression in combination with sorafenib treatment. Given the physiological role of SHP2 as a downstream effector of many RTKs, we hypothesized that SHP2 blockade may be a possible way to interrupt the positive feedback loop that causes RTK activation, leading to the development of acquired sorafenib resistance in HCC. Recently, a selective, potent and orally bioavailable small-molecule SHP2 inhibitor, SHP099, has been invented that inhibits SHP2, but not SHP1, activity through an allosteric mechanism.[12] A recent report has demonstrated the efficacy of SHP099 in the suppression of tumor growth of RAS-driven cancers, including breast and esophageal cancers.[12] Additionally, SHP099 activity synergized with the effect of MEK inhibitors (MEK-I) in a variety of types of cancers.[13-17] Thus far, the therapeutic efficacy of SHP099, alone and in combination with sorafenib, has not been examined in HCC.

In this study, we examined this hypothesis *in vitro* with HCC cells and primary HCC-derived organoid culture and *in vivo* with HCC xenograft and syngeneic models. Our results suggest that SHP2 inhibition could be a potential strategy to override sorafenib resistance, and the combination of sorafenib with SHP099 may be a novel therapeutic strategy against HCC.

Materials and Methods

Human HCC cell lines

MHCC-97L and MHCC-97H (Liver Cancer Institute, Fudan University, China), Huh7 and PLC/PRF/5 (Japan Cancer Research Bank, Tokyo, Japan), Hep3B, SNU182 and HepG2 (American Type Culture Collection) were maintained in DMEM containing high glucose (Gibco BRL) with 10% heat-inactivated fetal bovine serum (Gibco BRL), 100 mg/mL penicillin G, and 50 μg/mL streptomycin (Gibco BRL) at 37°C in a humidified atmosphere containing 5% CO_2. The immortalized normal liver cell line, MIHA, was kindly provided by Dr. J.R. Chowdhury, Albert Einstein College of Medicine, New York. All cell lines used in this study were obtained between 2013 and 2016, regularly authenticated by morphologic observation and AuthentiFiler STR (Invitrogen) and tested for the absence of mycoplasma contamination (MycoAlert, Lonza). Experiments were performed within 20 passages after cell thawing.

Establishment of sorafenib-resistant HCC cells

Sorafenib-resistant clones of Huh7, PLC/PRF/5 and MHCC-97L were established by subjecting HCC cells to continuous administration of gradually increasing sorafenib concentrations and were trained up to 8μM (Huh7) and 10μM (PLC/PRF/5 and MHCC-97L) respectively. Same volume of DMSO was added to the cells as mock controls during establishment of these resistant cells. Sorafenib-resistant PDTX#1 was established by administering sorafenib orally at 100mg/kg/day in NOD/SCID mouse bearing PDTX#1[18] for 25 days. Same treatment protocol was applied to the secondary mouse recipient. Successful establishment of sorafenib resistance was evidenced by an observation that there was no tumor suppression effect upon sorafenib treatment after two rounds of sorafenib administration.[19]

In vivo drug treatment assay

A total of 1 x 10^6 MHCC-97L and Huh7, while 0.5 x 10^6 patient derived tumor xenograft (PDTX) #PY003 and sorafenib-resistant PDTX#1 cells, were prepared according to the cell dissociation protocol in Supplementary Information and were injected into the flanks of BALB/C nude mice, NSG and NOD/SCID mice. Once the tumors were established and reached approximately 8 mm × 8 mm (length x

width), the mice were randomly divided into four groups: DMSO with 0.5% Tween 80/methylcellulose; DMSO and SHP099 (100mg/kg) (MedChemExpress), sorafenib (30mg/kg) (LC Laboratories) and the combined treatment group. SHP099 was resuspended in 0.5% methylcellulose with Tween80 in 0.9% saline. Sorafenib was dissolved in DMSO before diluting in water. The mice were given sorafenib orally on a daily basis, while SHP099 was given orally every other day. The tumor volume and body weight were measured every three days. The tumor volume was calculated using the following formula: volume (cm^3) = $L \times W^2 \times 0.5$. The mice were treated for 21 days before sacrifice (while Huh7 xenograft for 23 days), at which point tumors were harvested for analysis. The study protocol was approved by and performed in accordance with the Committee of the Use of Live Animals in Teaching and Research at the University of Hong Kong and the Hong Kong Polytechnic University.

Statistical analysis

The statistical significance of the results obtained from qRT-PCR, sphere formation assays, and flow cytometry analysis was determined by GraphPad Prism. All qRT-PCR, flow cytometry, immunohistochemistry staining, *in vivo* tumor volume experimental data were analyzed using *t*-test or Mann–Whitney's *U*-test wherever appropriate. The results are shown as the means and standard deviations, and p-values less than 0.05 were considered statistically significant (* $p<0.05$, ** $p<0.01$, *** $p<0.001$ & ****$p<0.0001$). Kaplan-Meier survival analysis was used to examine the tumor-free survival of immune-competent mouse model after SHP099 and/or sorafenib treatment. The statistical significance was calculated by log-rank test.

Additional experimental procedures are provided in the Supplementary Information.

Results

Upregulation of RTKs and their positive effector SHP2 was observed in sorafenib-resistant HCC cells

A previous study showed that SHP2 is a potential predictive biomarker for sorafenib response.[10] To further correlate the SHP2 expression of HCC cells to sorafenib response *in vitro*, we first determined the expression levels of SHP2 in a panel of HCC cell lines (Supplementary Fig. S1). Next, we examined the IC_{50} values of these HCC cell lines upon sorafenib treatment. HCC cells with higher SHP2 expression showed a lower sensitivity towards sorafenib treatment (Supplementary Fig. S2A). The regulatory role of SHP2 in sorafenib resistance was further evidenced by upregulation of SHP2 mRNA and protein levels in our established sorafenib-resistant HCC cell lines, including Huh7, PLC/PRF/5, MHCC-97L cells and PDTX#1[18] when compared to that of controls (Fig. 1A&B). By performing human phospho-RTK array, we consistently found that phosphorylation levels of several known targets of sorafenib including FGFR1, 2α, 3, 4, PDGFRβ, VEGFR1 and VEGFR2 were commonly downregulated (Supplementary Fig. S3), while phosphorylation levels of several RTKs, including AXL, EGFR, EPHA2, and IGF1R were commonly upregulated in two sorafenib resistant HCC cells when compared with mock controls (Fig. 1C). To further confirm our hypothesis that RTK reactivation is crucial for the adaptive resistance mechanism of HCC cells in response to sorafenib treatment, we compared the gene expression of various RTKs between sorafenib-resistant HCC cells and their control counterparts. By qRT-PCR analysis, we identified a negative feedback mechanism via RTKs, as shown by the increase in the expression of multiple RTKs, including AXL, EGFR, ERBB2, FGFR1, IGF1R and InsulinR, in sorafenib-resistant HCC cells, as compared to controls (Fig. 1D).

SHP099 overrides the adaptive resistance to sorafenib in vitro

To explore the effect of SHP099 on HCC cells, we chose high SHP2 expressing Huh7, PLC/PRF/5 and MHCC-97L cells for testing its drug efficacy (Supplementary Fig. S1). These three cell lines are RTK-dependent cell lines without BRAF and KRAS mutations. By using MTT assay, among the seven HCC cell lines being examined, we found that SHP099 suppressed the growth of these three HCC cell lines in a dose-dependent manner with the highest IC_{50} values of 32.48μM, 66.77μM and

42.9μM, respectively (Fig. 2A & Supplementary Table S1). Upon analysis, we found that IC_{50} values of SHP099 correlated with SHP2 expression in HCC cells (Supplementary Fig. S2B). Apart from HCC cell lines, the IC_{50} values of cell lines of other tumor types was also examined for comparison (Supplementary Table S1). Next, we examined the combined effect of SHP099 with sorafenib in these three HCC cell lines. By Annexin V apoptosis assay, SHP099 at low doses (10μM-30μM) sensitized Huh7, PLC/PRF/5, MHCC-97L, Hep3B, SNU182 and HepG2 cells to the effect of sorafenib treatment (Fig. 2B & Supplementary Fig. S4). By Bliss Independence Analysis, SHP099 in combination with sorafenib showed synergistic induction of apoptosis in all these HCC cell lines (Supplementary Table S2). Apart from the increase in the percentage of apoptosis, the combination-treated HCC cells exhibited senescence, as shown by the increase in senescence-associated β-galactosidase and expression of p21, in a synergistic manner in Huh7 and PLC/PRF/5 cells (Fig. 2C&D & Supplementary Table S3). To further examine the effect of SHP099 on the reversal of sorafenib resistance in HCC cells, we analyzed the effect of SHP099 in combination with sorafenib in sorafenib-resistant Huh7 and PLC/PRF/5 cells. Consistently, we found that sorafenib-resistant Huh7 and PLC/PRF/5 cells showed fewer apoptotic cells than mock control cells upon administration of sorafenib (Fig. 2E). More strikingly, SHP099 synergistically reversed the resistance phenotype of sorafenib-resistant Huh7 and PLC/PRF/5 cells (Fig. 2E & Supplementary Table S2).

SHP099 abrogated sorafenib-induced reactivation of the MEK/ERK and AKT pathways

Since SHP2 acts upstream of RAS in various RTK signaling pathways, we first analyzed the activation status of RAS in sorafenib-resistant cells. Consistently, we observed an increase in RAS-GTP levels in sorafenib-resistant Huh7 and PLC/PRF/5 cells by RAS pull down assay (Fig. 3A) compared to control cells. SHP2 is required for RTK-induced RAS activation, resulting in the activation of the MEK/ERK and AKT pathways.[20,21] Therefore, we also examined the phosphorylation status of MEK, ERK and AKT in sorafenib-resistant cells. Consistently, we found increased expression of p-MEK, p-ERK, and p-AKT in sorafenib-resistant HCC cells (Fig. 3B) compared to control cells. Further, we assessed the effect of sorafenib alone and in combination with SHP099 on RAS activation after prolonged (48 hours) treatment. After 48 hours, RAS activation was

drastically increased in sorafenib-treated cells (Fig. 3C) compared to controls. Notably, this increase was abrogated upon administration of SHP099 (Fig. 3C). To understand the underlying mechanism, we treated HCC cells with sorafenib or SHP099 alone and in combination for 2 hours, 4 hours, 24 hours and 48 hours. Consistent with the suppressive role of sorafenib on Raf/MEK/ERK signaling, we found that sorafenib blocked the phosphorylation of MEK, ERK, and AKT after 2 to 4 hours of treatment, but the phosphorylation levels progressively rebounded from 24 hours to 48 hours. Interestingly, the adaptive increase in MEK/ERK and AKT activity was abolished by co-administration of SHP099 (Fig. 3D). This result showed that there were progressive and dynamic changes in the MEK/ERK and AKT signaling pathways upon treatment with sorafenib alone or in combination with SHP099. This observation was also observed in sorafenib-resistant Huh7 and PLC/PRF/5 cells upon combination treatment (Fig. 3E). To further confirm the effect of SHP099 on the downregulation of the sorafenib-induced MEK/ERK pathway, we specifically examined ERK1/2-dependent gene expression by qRT-PCR analysis. Similar to the dynamic changes in the phosphorylation levels of MEK/ERK, we observed concurrent increases in DUSP6, ETV1, ETV5, FOSL1, and SPRY2 upon 48-hour sorafenib treatment, and their expression was strongly inhibited by the combination treatment (Fig. 3F), which the increase in ERK1/2-dependent gene expression was also observable in sorafenib-resistant cells. Lastly, the negative feedback mechanism that involved RTKs was also supported by the increase in RTK expression, including EGFR, FGFR1, FGFR2, IGF1R and MET, upon sorafenib treatment (Supplementary Fig. S5). Collectively, the above data suggested that SHP099 abrogated sorafenib-induced reactivation of the RTK-mediated MEK/ERK and AKT pathways.

Suppression of SHP2 effectively enhances the effect of sorafenib in organotypic ex vivo human HCC clinical samples

In light of the synergistic effect of SHP099 with sorafenib treatment, we extended our study to examine the effect of SHP099 alone and in combination with sorafenib in a more clinically relevant setting by performing organotypic *ex vivo* culture of primary HCC tumor samples. HCC patient-derived organoids have been thoroughly characterized at both molecular and histological levels, with comparisons made against the original tissue samples.[22] These HCC organoids were found to be

SHP2 positive by immunohistochemistry (Fig. 4A & Supplementary Fig. S6A). The treatment efficacy of sorafenib and SHP099 was evaluated in this *ex vivo* culture of HCC patient-derived organoids treated with either SHP099, sorafenib, or the combination of the two. Using a CellTiter-Glo assay, we found that combination treatment resulted in the most significant reduction in tumor cell growth and that SHP099 treatment sensitized HCC cells to sorafenib (Fig. 4B&C & Supplementary Fig. S6B). This was accompanied by the consistent inhibition of the phosphorylation levels of MEK, ERK, and AKT (Fig. 4D). Apart from the suppression of HCC cell growth, the combination-treated HCC cells also exhibited enhanced apoptosis, as evidenced by the TUNEL assay as compared to single-agent treatment and mock controls (Fig. 4E).

SHP099 combined with sorafenib results in maximal tumor growth suppression in HCC xenograft models

We examined the therapeutic effect of SHP099 alone and its combined effect with sorafenib *in vivo* using HCC xenografts derived from MHCC-97L and (PDTX) #PY003 cells. Treatment was started once the size of the xenograft reached approximately 8mm × 8 mm (length x width). The mice were separated into the following four subgroups: (i) DMSO with 0.5% Tween 80/methylcellulose; (ii) DMSO and SHP099 (100mg/kg) (MedChemExpress); (iii) sorafenib (30mg/kg) and control 0.5% Tween 80/methylcellulose; and (iv) SHP099 and sorafenib. The tumors and their corresponding volumes are shown in Fig. 5A&B after treatment for 21 days. SHP099 reduced the tumor volumes in a manner similar to that of sorafenib. In addition, SHP099 combined with sorafenib exerted a synergistic effect, resulting in maximal suppression of tumor growth compared with that of the control group. Strikingly, we found that this combination treatment markedly reduced the tumor volumes of MHCC-97L and PY003 by 79% and 38%, respectively, relative to the original tumor volume on Day 0 (Fig. 5C, Supplementary Fig. S7). During this experiment, no signs of toxicity (infection, diarrhea, damage to vital organs or loss of body weight) were observed in the animals undergoing combination treatment (Supplementary Fig. S8). Consistent with these biological effects, we observed suppression of the phosphorylation levels of ERK and AKT in the combination treatment group (Fig. 5D). In addition, we found that combination treatment greatly suppressed cell proliferation, as evidenced by the decrease in PCNA staining as compared to single-agent treatment

and mock controls (Fig. 5D). In addition, combination treatment generated a suppressive effect on angiogenesis, with a decrease in CD31 staining (Fig. 5D). In addition, we also evaluated this combination strategy in HCC xenografts derived from Huh7, and similar tumor suppressive effects were observed after combined treatment (Supplementary Fig. S9). It is crucial to evaluate whether a similar result is obtained in HCC isolated from sorafenib non-responders. For this purpose, we evaluated their combinatorial effects in the sorafenib-resistant PDTX#1.[18] Similarly, we found that SHP099/sorafenib exerted the greatest tumor suppressive effects when compared with the single-agent treatment and mock controls (Fig. 5E).

Inhibition of SHP2 sensitized HCC cells to sorafenib treatment in an immune-competent mouse model

Recently, SHP2 was found to critically mediate the inhibitory effect of PD-1 in T cells upon binding to its ligand PD-L1 in APCs.[23] Based on these data, the blockade of SHP2 by SHP099 may lead to T cell activation. Given the activation of both the RAS/MAPK and PI3K/AKT/mTOR pathways in almost 50% of HCC patients,[24] we utilized sleeping beauty transposase to introduce activated forms of NRAS and AKT by hydrodynamic transfection (HT) to examine the effect of the combination of SHP099 and sorafenib in a sorafenib-refractory immune-competent mouse model[19] (Fig. 6A). Upon the HT of plasmids, we started to treat mice with sorafenib at 30mg/kg for 20 days. This resembles the clinical situation in which sorafenib nonresponsive patients with HCC progress after sorafenib treatment. At this point, the mice in a group of 11-12 were divided into 4 groups with the same treatment as is shown in Fig. 6A. The efficacy of the combined drug treatment was evaluated by the liver weight over body weight ratio and was compared to the single-drug treatment groups. We found that SHP099/sorafenib led to significantly improved survival and the maximal suppression of tumor growth, indicating that SHP099 treatment can synergize with sorafenib treatment and is effective against liver tumors *in vivo* (Fig. 6B-D). The decrease in tumor volume paralleled the decrease in PCNA, CD31, p-ERK and p-AKT and staining levels (Fig. 6E). To examine the effect of the combination treatment on T cells infiltration, we first examined the intra-tumor expression of CD3 in four groups of mice. As shown in Supplementary Fig. S10, we found that tumor treated by SHP099

alone and combo therapy showed highest intra-tumor CD3 expression, as compared to sorafenib alone and mock control.

Discussion

Our previous report showed that SHP2 played a crucial role in the regulation of sorafenib resistance in HCC cells.[10] Consistent with this finding, we found that SHP2 was upregulated in our established sorafenib-resistant HCC cells. In HCC, the functions of SHP2 was found to be bi-directional. In $Shp2^{hep-/-}$ mice, SHP2 was found to exert tumor-suppressive role in HCC initiation,[25] while expression of SHP2 was overexpressed in human HCCs and correlated with HCC progression.[11] Recently, Kang et al., have reported that SHP2 transcript levels was upregulated in HBX-transfected HCC cells via NF-κB activation.[26] Mechanistically, SHP2 expression was induced through direct binding of NF-κB on its promoter. Since NF-κB activation was reported to be crucial in HCC [26] and sorafenib resistance,[18] its activation may be one of the possible mechanisms leading to SHP2 upregulation in both parental and sorafenib-resistant HCC cells. SHP2 was first identified as an oncogenic tyrosine phosphatase that contains two Src-homology 2 domains in the early 1990s.[27] Unlike other tyrosine phosphatases, SHP2 functions as a positive regulator of proliferative signals. Substantial genetic and biochemical evidence has shown that SHP2 is an important component of RTK signaling, including FGFR, VEGFR, PDGFR and EGFR signaling in response to various growth factors, leading to full activation of extracellular signal-regulated kinase signaling[28] and the PI3K/AKT/mTOR pathway.[29] In this study, we observed the upregulation of various RTKs in sorafenib-resistant HCC cells. Given the physiological role of SHP2 as a downstream effector of many RTKs, our data showed that SHP2 blockade may be a way to interrupt the negative feedback pathway via RTK activation that leads to the development of acquired sorafenib resistance in HCC. Recently, blockade of SHP2 showed growth suppression in RTK-dependent cancer cells.[12,30] We found here that SHP099 not only induced apoptosis of HCC cells but also exerted a synergistic effect with sorafenib on RTK-dependent HCC cells. Most importantly, SHP099 reversed the resistance phenotype of sorafenib-resistant HCC cells. Similarly, suppression of SHP2 was found to enhance the effects of MEK-I and crizotinib in resistant cancer cells of PDAC and ALK-mutant NSCLC cells.[16,31] In addition to the enhanced apoptotic effect, we found that the SHP099/sorafenib combination led to the cellular senescence of HCC cells. These data further support the role of SHP2 in the suppression of senescence in mammary gland cancer in mice.[32]

We observed RAS activation in sorafenib-resistant and sorafenib-treated HCC cells, which was accompanied by increased RTK signaling. Blockade of SHP2 by SHP099 suppressed the adaptive increase in RAS activation in sorafenib-treated HCC cells. This is in line with a study by Fedele et al., which showed a suppressive effect on RAS activity in MEK-I-treated cells.[16] In addition, the authors also demonstrated that SHP099 also decreased mutant RAS activation in multiple KRAS-mutant PDAC lines.[16] SHP2 is required for RTK-evoked RAS activation, resulting in the activation of the MEK/ERK and AKT pathways.[20,21] Consistently, we found that SHP099 strongly impeded the adaptive activation of the MEK/ERK and AKT pathways in sorafenib-treated HCC cells. However, we did not observe consistent results on the suppression of p-STAT3 upon SHP099 treatment (data not shown). Our observation is consistent with the data showing the suppression of the ERK and AKT pathways in cancers of lung and pancreas upon SHP099 treatment.[13,16] In addition, we found that many RTKs, including EGFR, FGFR1, FGFR2, IGF1R and MET, were upregulated, while their expression was drastically decreased upon inactivation of SHP2 by SHP099. Recently, there was a report showing that FGFR could drive adaptive resistance to RAF and MEK inhibitors independently of SHP2.[33] The dependence of SHP2 on adaptive resistance may be drug dependent.

We examined the therapeutic efficacy of SHP099 in combination with sorafenib by oral gavage in xenograft models derived from MHCC97L and PY003. After 21 days, SHP099/sorafenib treatment markedly reduced the tumor volume of MHCC-97L and PY0033 by 79% and 38%, when compared with the original size at Day 0. This tumor reduction effect was also reported in PDAC and TNBC models when SHP099 was combined with MEK-I.[16] Accompanied with this phenotypic change, we found combo treatment led to drastic decrease in phosphorylation levels of p-ERK and p-AKT. Interestingly, we found that combo treatment suppressed angiogenesis, as evidenced by the decrease in CD31 staining. Since SHP2 was reported to play crucial role in mediating the inhibitory function of PD1 in T cells,[23] we would like to examine whether SHP099/sorafenib treatment will exert enhancing effect on T cells. For this purpose, we employed sorafenib-refractory immune-competent mouse model by introducing activated forms of NRAS and AKT by HT. We found that SHP099/sorafenib led to maximal suppression of tumor growth with significantly improved survival rate. Interestingly, we found enhanced T cell infiltration in both SHP2 alone and combo treatment,

which implicates the potential role of SHP099 in modulation of T cells for immune cancer therapy. Having said that, the tumor suppressive effect in this HT model is not as drastic as observed in xenografts. This is possibly due to the fact that AKT is constitutively active in this model while SHP099 might not effectively suppress its activation.

In conclusion, we have demonstrated that SHP2 blockade can impede the sorafenib-induced reactivation of the ERK/MAPK and AKT pathways, possibly via an RTK feedback mechanism (Supplementary Fig. S11). Targeting SHP2 by SHP099 in combination with sorafenib may be a novel and safe therapeutic strategy against HCC.

Acknowledgements

We thank the University Research Facility in Life Sciences (Hong Kong Polytechnic University) and the Faculty Core Facility (University of Hong Kong) for providing and maintaining the equipment and technical support needed for flow cytometry analysis and imaging microscopy (Hong Kong Polytechnic University and University of Hong Kong) for help with sectioning as well as the Centralized Animal Facility (Hong Kong Polytechnic University) and the Laboratory Animal Unit (University of Hong Kong) for supporting our animal studies. We thank Dr. Xin Chen (University of California, San Francisco) for sharing of plasmids used for hydrodynamic tail vein injection. We thank Dr. Meritxell Huch (The Gurdon Institute, University of Cambridge) for sharing of her HCC organoids.

References

1. Bray F, Ferlay J, Soeriomataram I, Siegel RL, Torre LA, Jermal A. Global cancer statistics 2018: GLOBOCAN estimates of incidence and mortality worldwide for 36 cancers in 185 countires. CA Cancer J Clin 2018;68:394-424.
2. Llovet JM, Di Bisceglie AM, Bruix J, Kramer BS, Lencioni R, Zhu AX, et al. Design and endpoints of clinical trials in hepatocellular carcinoma. J Natl Cancer Inst 2008;100:698-711.
3. Llovet JM, Ricci S, Mazzaferro V, Hilgard P, Gane E, Blanc JF, et al. Sorafenib in advanced hepatocellular carcinoma. N Engl J Med 2008;359:378-390.
4. Cheng AL, Kang YK, Chen Z, Tsao CJ, Qin S, Kim JS, et al. Efficacy and safety of sorafenib in patients in the Asia-Pacific region with advanced hepatocellular carcinoma: a phase III randomised, double-blind, placebo-controlled trial. Lancet Oncol 2009;10:25-34.
5. Yau T, Yao TJ, Chan P, Wong H, Pang R, Fan ST, et al. The significance of early alpha-fetoprotein level changes in predicting clinical and survival benefits in advanced hepatocellular carcinoma patients receiving sorafenib. Oncologist 2011;16:1270-1279.
6. Donev IS, Wang W, Yamada T, Li Q, Takeuchi K, Matsumoto K, et al. Transient PI3K inhibition induces apoptosis and overcomes HGF-mediated resistance to EGFR-TKIs in EGFR mutant lung cancer. Clin Cancer Res 2011;17:2260-2269.
7. Yang L, Li J, Ran L, Pan F, Zhao X, Ding Z, et al. Phosphorylated inuslin-like growth factor 1 receptor is implicated in resistance to the sytostatic effect of gefitinib in colorectal cancer cells. J Gastrointest Surg 2011;15:942-957.
8. Zhai B, Hu F, Jiang X, Xu J, Zhao D, Liu B, et al. Inhibition of Akt reverses the acquired resistance to sorafenib by switching protective autophagy to autophagic cell death in hepatocellular carcinoma. Mol Cancer Ther 2014;13:1589-1598.
9. Chen J, Ji T, Zhao J, Li G, Zhang J, Jin R, et al. Sorafenib-resistant hepatocellular carcinoma stratified by phosphorylated ERK activates PD-1 immune checkpoint. Oncotarget 2016;7:41274-41284.
10. **Xiang D**, **Cheng Z**, **Liu H**, **Wang X**, Han T, Sun, W, et al. SHP2 promotes liver cancer stem cell expansion by augmenting β-cateinin signaling and predicts chemotherapeutic response of patients. Hepatology 2017;65:1566-1580.

11. **Han T**, **Xiang DM**, **Sun W**, **Liu N**, Sun HL, Wen W, et al. PTPN11/Shp2 overexpression enhances liver cancer progression and predicts poor prognosis of patients. J Hepatol 2015;63:651-660.
12. Chen YN, LaMarche MJ, Chan HM, Fekkes P, Garcia-Fortanet J, et al. Allosteric inhibition of SHP2 phosphatase inhibits cancers driven by receptor tyrosine kinases. Nature 2016;535:148-152.
13. Wong GS, Zhou J, Liu JB, Wu Z, Li T, Xu D, et al. Targeting wild-type KRAS-amplified gastroesophageal cancer through combined MEK and SHP2 inhibition. Nat Med 2018;24:968-977.
14. Ruess DA, Heynen GJ, Ciecielski KJ, Ai J, Berninger A, Kabacaogiu D, et al. Mutant KRAS-driven cancers depend on PTPN11/SHP2 phosphatase. Nat Med 2018;24:954-960.
15. Mainardi S, Mulero-Sánchez A, Prahallad A, Germano G, Bosma A, Krimpenfort P, et al. SHP2 is required for growth of KRAS-mutant non-small lung cancer *in vivo*. Nat Med 2018;24:961-967.
16. Fedele C, Ran H, Diskin B, Wei W, Jen J, Geer MJ, et al. SHP2 inhibition prevents adaptive resistance to MEK inhibitors in multiple cancer models. Cancer Discov 2018;8:1237-1249.
17. Nichols RJ, Haderk F, Stahlhut C, Schulze CJ, Hermmati G, Wildes D, et al. RAS nucleotide cycling underlies the SHP2 phosphatase dependence of mutant BRAF-, NF1- and RAS-driven cancers. Nat Cell Biol 2018;20:1064-1073.
18. Lo J, Lau EY, Ching RH, Cheng BY, Ma MK, Ng IO, et al. Nuclear factor kappa B-mediated CD47 upregulation promotes sorafenib resistance and its blockade synergizes the effect of sorafenib in hepatocellular carcinoma in mice. Hepatology 2015;62:534-545.
19. Tong M, Che N, Zhou L, Zhou L, Luk ST, Kau PW, et al. Efficacy of annexin A3 bloackade in sensitizing hepatocellular carcinoma to sorafenib and regorafenib. J Hepat 2018;69:826-839.
20. Ran H, Tsutsumi R, Araki T, Neel BG. Sticking It to Cancer with Molecular Glue for SHP2. Cancer Cell 2016;30:194-196.
21. Chan. G, Neel BG. Role of PTPN11 (SHP2) in Cancer. Protein Tyrosine Phosphatases in Cancer. New York: Springer, 2016:115-143.

22. **Chan LH**, **Zhou L**, **Ng KY**, **Wong TL**, Lee TK, Sharama R, et al. PRMT6 regulates RAS/RAF binding and MEK/ERK-mediated cancer stemness activities in hepatocellular carcinoma through CRAF methylation. Cell Rep 2018;25:690-701.
23. Hui E, Cheung J, Zhu J, Su X, Taylor MJ, Wallweber HA, et al. T cell costimulatory receptor CD28 is a primary target for PD-1-mediated inhibition. Science 2017;355:1428-1433.
24. Llovet JM, Villanueva A, Lachenmayer A, Finn RS. Advances in targeted therapies for hepatocellular carcinoma in the genomic era. Nat Rev Clin Oncol 2015;12:408-424.
25. Brad-Chapeau EA, Yuan J, Droin N, Long S, Zhang EE, Nyuyen TV, et al. Ptpn11/shp2 acts as a tumor suppressor in hepatocellular carcinogenesis. Cancer Cell 2011;19:629-639.
26. Kang HJ, Chung DH, Sung CO, Yoo SH, Yu E, Kim N, et al. SHP2 is induced by the HBx-NF-κB pathway and contributes to fibrosis during human early hepatocellular carcinoma development. Oncotarget 2017;8:27263-27276.
27. Mohi MG, Williams IR, Dearolf CR, Chan G, Kutok JL, Cohen S, et al. Prognostic, therpaeutic and mechanistic implications of a mouse model of leukemia evoked by Shp2 (PTPN11) mutations. Cancer Cell 2005;7:179-191.
28. Zhang SQ, Yang W, Kontarridis ML, Bivona TG, Wen G, et al. Shp2 regulates SRC family kinase activity and Ras/Erk activation by controlling Csk recruitment. Mol Cell 2004;13:341-355.
29. Yang X, Tang C, Luo H, Wang H, Zhou X. Shp2 confers cisplatin resistance in small cell ung cancer via an AKT-mediated increase in CA916798. Oncotarget 2017;8:23664-23674.
30. Garcia Fortanet J, Chen CH, Chen YN, Chen Z, Deng Z, Firestone B, et al. Allosteric Inhibition of SHP2: Identification of a Potent, Selective, and Orally Efficacious Phosphatase Inhibitor. J Med Chem 2016;59:7773-7782.
31. Dardaei L, Wang HQ, Singh M, Fordjour P, Shaw KX, Yoda S, et al. SHP2 inhibition restores sensitivity in ALK-rearranged non-small-cell lung cancer resistant to ALK inhibitors. Nat Med 2018;24:512-517.
32. Lan L, Holland JD, Qi J, Fordjour P, Shaw KX, Yoda S, et al. Shp2 signaling suppresses senescence in PyMT-induced mammary gland cancer in mice. EMBO J 2015;34:1493-1508.

33. Ahmed TA, Adamopoulos C, Karoulia Z, Wu X, Sachidanandam R, Arronson SA, et al. SHP2 drives adaptive resistance to ERK signaling inhibition in molecularly defined subsets of ERK-dependent tumors. Cell Rep 2019;26:65-78.

Figure Legends

Fig. 1. SHP2 upregulation and RTK reactivation in sorafenib-resistant HCC cells. (A) Upregulation of *SHP2* mRNA in sorafenib-resistant HCC cells, as determined by qRT-PCR (*p<0.05 & ** p<0.01, *t* test). **(B)** Confirmation of the upregulation of SHP2 protein in sorafenib-resistant cells derived from Huh7, PLC/PRF/5, MHCC-97L and PDTX#1 by western blot analysis. **(C)** Upregulation of phosphorylation of RTKs were detected using human phospho-RTK arrays in sorafenib-resistant HCC cells. **(D)** Alterations in the expression of various RTKs in sorafenib-resistant HCC cells, as determined by qRT-PCR (*p<0.05, ** p<0.01, ***p<0.001 & **** p<0.0001, *t* test). Error bars represent the standard deviation (SD) from at least three independent experiments.

Fig. 2. SHP099 sensitized HCC cells to the effect of sorafenib. (A) IC_{50} values of SHP099 for Huh7, PLC/PRF/5 and MHCC-97L cells were determined by MTT assay. The data shown are from two independent experiments. **(B)** Inhibition of SHP2 by SHP099 significantly sensitized Huh7, PLC/PRF/5 and MHCC-97L cells to the effect of sorafenib (*p<0.05, **p <0.01 & ***p<0.001, *t* test). **(C)** Representative images of SA-β-gal staining of HCC cells treated with DMSO, sorafenib (Huh7: 8μM, PLC/PRF/5 & MHCC-97L: 10μM), SHP099 (Huh7: 10μM, PLC/PRF/5: 30μM & MHCC-97L: 20μM), or both drugs for 48 hours. Scale bar: 20μm. (**p<0.01 & ***p<0.001, *t* test). **(D)** Immunoblots of whole cell lysates for p21 in indicated cells upon drug treatment for 48 hours. **(E)** The apoptotic effect of SHP099/sorafenib in sorafenib-resistant Huh7 and PLC/PRF/5 cells was determined by Annexin V staining. (*p<0.05 & **p<0.01, *t* test).

Fig. 3. SHP099 inhibited RAS to impede the adaptive resistance of sorafenib via RTK-mediated MEK/ERK and AKT reactivation. (A) Immunoblots of whole cell lysates or RAF-RBD-precipitated lysate from sorafenib-resistant Huh7 and PLC/PRF5 cells, which showed increased RAS-GTP levels when compared with mock control cells. Band intensity was quantified by Image J. **(B)**

Increased levels of p-MEK1/2, p-ERK1/2 and p-AKT(Ser473) were observed in sorafenib-resistant Huh7 and PLC/PRF/5 cells. **(C)** Immunoblots of whole cell lysates or RBD-precipitated lysate from HCC cells treated with DMSO, sorafenib (Huh7: 8μM, PLC/PRF/5 & MHCC-97L: 10μM), SHP099 (Huh7: 10μM, PLC/PRF/5: 30μM & MHCC-97L: 20μM), or both drugs for 48 hours. The images shown are representative of at least two independent experiments. Band intensity was quantified by Image J. **(D)** HCC cells were incubated with sorafenib or SHP099 alone and in combination for 2 hours, 4 hours, 24 hours and 48 hours. Immunoblots of whole cell lysates for p-MEK1/2, p-ERK1/2 and p-AKT(Ser473) and their corresponding total protein levels. The image shown is representative of three independent biological replicates. **(E)** Sorafenib-resistant Huh7 and PLC/PRF/5 cells were treated as indicated for 48 hours. **(F)** Expression of ERK-dependent genes in HCC cells treated as indicated was assessed by qRT-PCR (*p<0.05, **p<0.01, ***p<0.001 & ****p<0.01, *t* test).

Fig. 4. The effect of SHP099/sorafenib treatment in suppressing tumor growth using organotypic *ex vivo* human HCC clinical samples. (A) Immunohistochemical analysis of SHP2 in a patient-derived organoid culture (HK-HCC P1). Scale bar: 100μm. **(B&C)** Percentage of growth in HCC patient-derived organoid culture #1, which was treated with DMSO, sorafenib (8μM), SHP099 (10μM) or sorafenib/SHP099 (combo) for 6 days (**p<0.01 & ***p<0.001). Scale bar: 0.25 mm. **(D)** Immunoblots for the expression of p-MEK1/2, p-ERK1/2 and p-AKT(Ser473) and their corresponding total protein levels in the indicated organoid culture HK-HCC P1. **(E)** TUNEL staining for apoptotic cells in organoid culture HK-HCC P1 for the indicated treatment and time (***p<0.001). Scale bar: 100μm.

Fig. 5. The effect of SHP099/sorafenib treatment in suppressing tumor growth in HCC xenografts. (A) Response of MHCC-97L and PY003 xenografts to treatment with SHP099 (100mg/kg), sorafenib (30mg/kg) or both drugs (SHP099 100mg/kg; sorafenib 30mg/kg). The tumor at the end of the treatment is shown. Scale bar: 1cm. **(B)** Graph showing the weight of tumors at the end of the treatment. (**p<0.01, ***p<0.001 & ****p<0.001, Mann-Whitney's U test). **(C)** Waterfall plot showing the response of each tumor after 21 days (*p<0.05 & **p<0.01, Mann-Whitney's U test). **(D)** Immunohistochemical images of p-ERK1/2, p-AKT(Ser473), PCNA and CD31 on resected

tumors. Scale bar: 100μm. Protein expression was quantified using ImageJ software. **(E)** Tumor growth curve and waterfall plot showing the response of each tumor from sorafenib-resistant PDTX#1 xenograft after 21 days treatment (*p<0.05 & **p<0.01, Mann-Whitney's U test).

Fig. 6. The effect of SHP099/sorafenib treatment in suppressing tumor growth in an immune-competent mouse model. (A) Schematic diagram of the treatment regimen with SHP099, sorafenib, or the combination of SHP099 with sorafenib. **(B)** Representative images of HCC tumors derived from the four groups at the endpoint are shown. Scale bar: 1cm. **(C)** Graphs showing the liver/body weight ratio generated from mice that died in each treatment group. (**p <0.01, *t* test). **(D)** Kaplan-Meier survival curves showing the percentage of tumor-free survival of each annotated group. $n = 11$-12 per group. Survival analysis in the mouse model was performed by log-rank test. **(E)** Immunohistochemical images of PCNA, CD31, p-ERK1/2 & p-AKT(Ser473) on resected tumors. Scale bar: 100μm. Protein expression was quantified using ImageJ software.

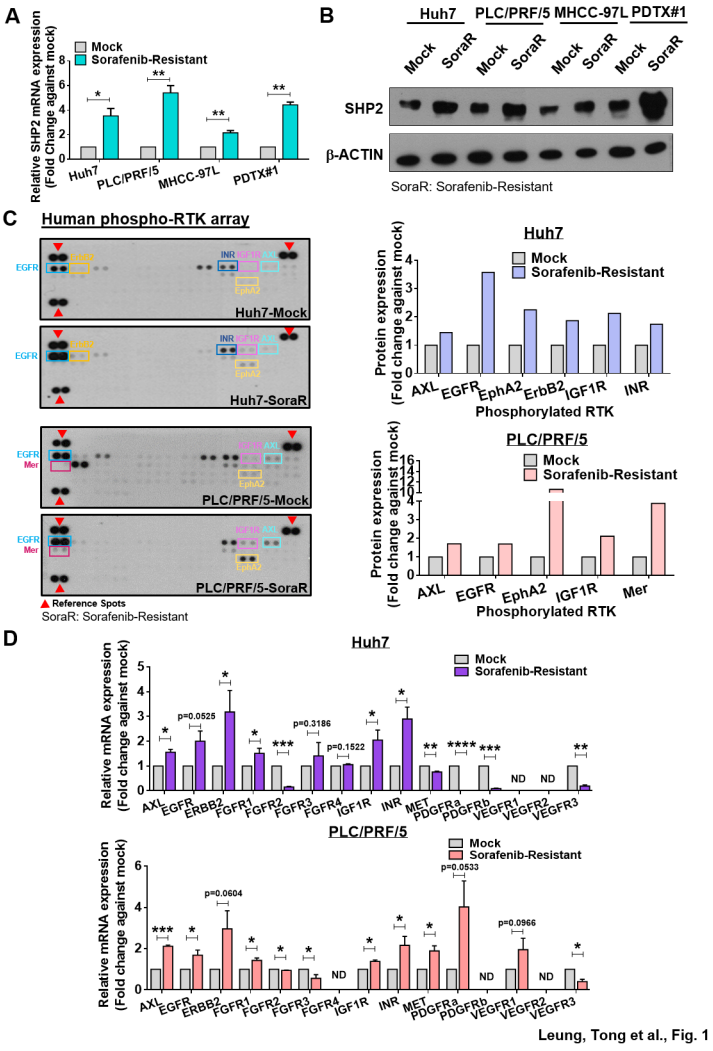

Leung, Tong et al., Fig. 1

hep_30989_f1.tif

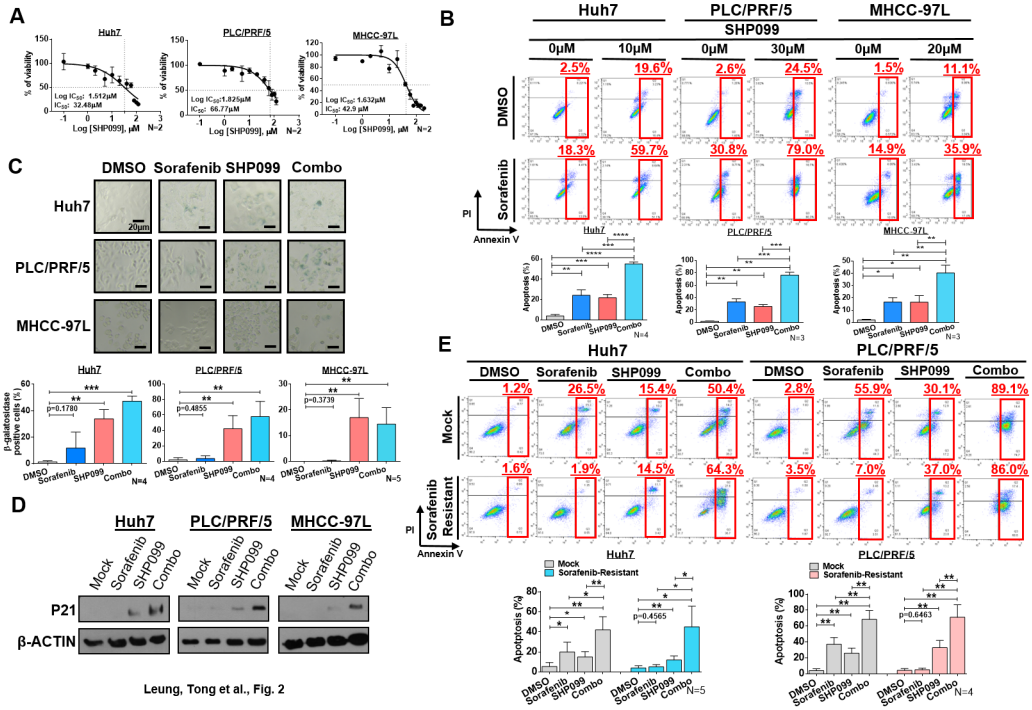

Leung, Tong et al., Fig. 2

hep_30989_f2.tif

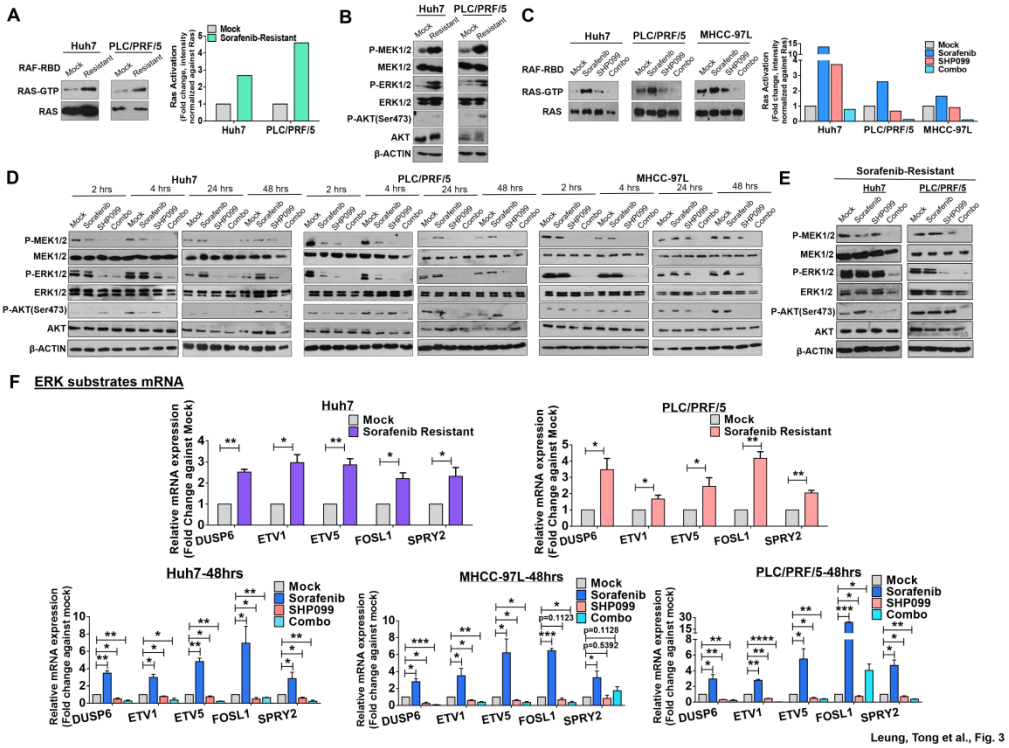

hep_30989_f3.tif

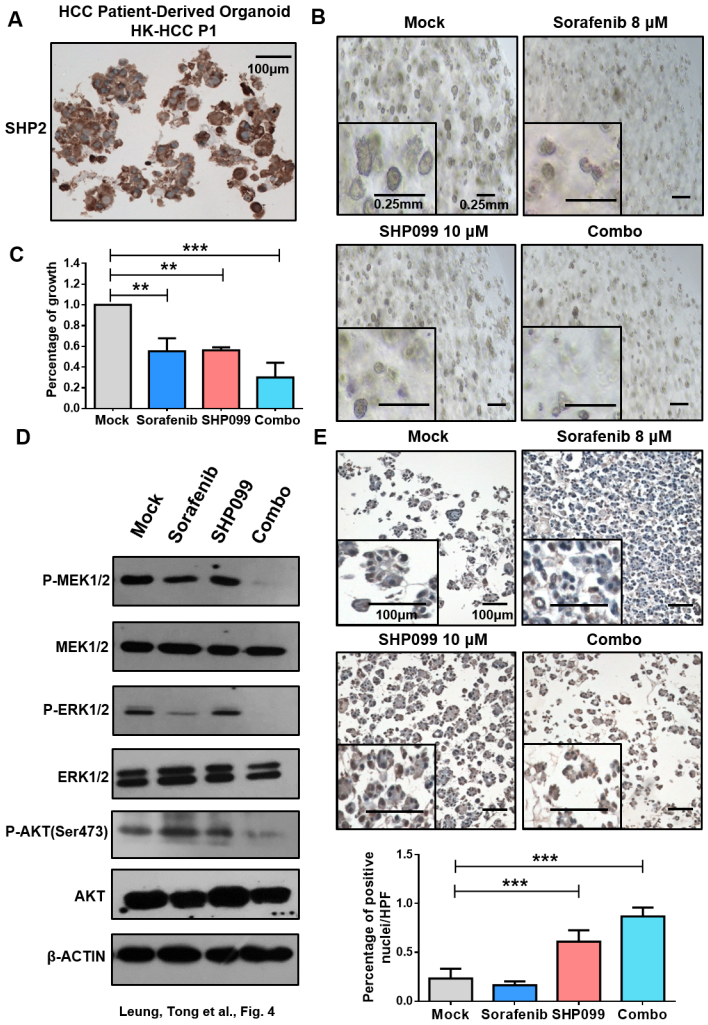

hep_30989_f4.tif

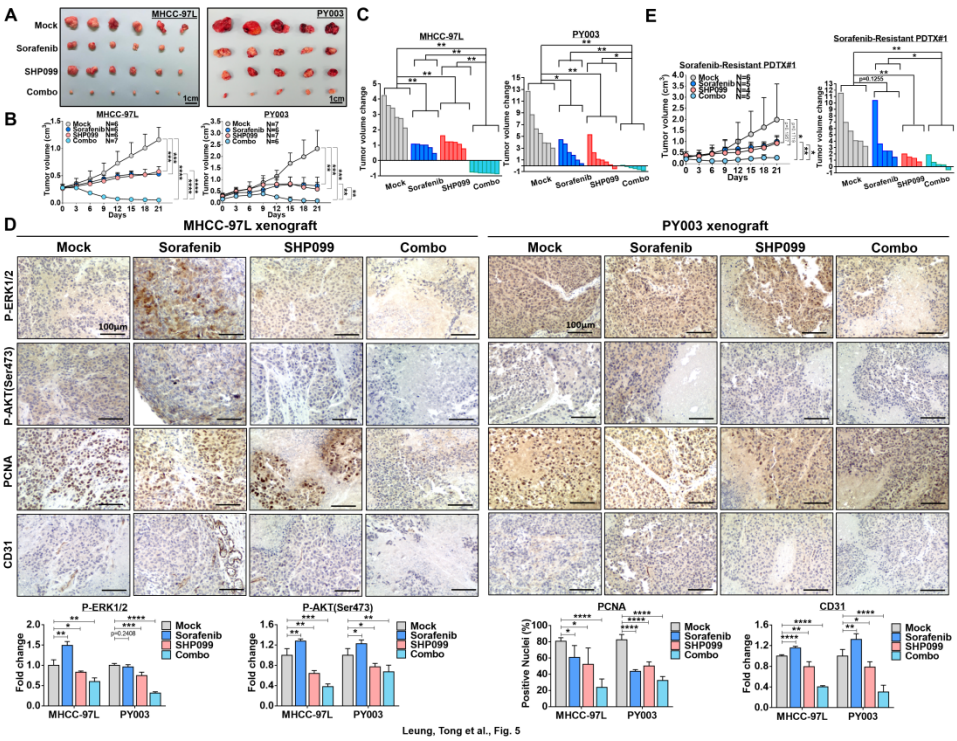

hep_30989_f5.tif

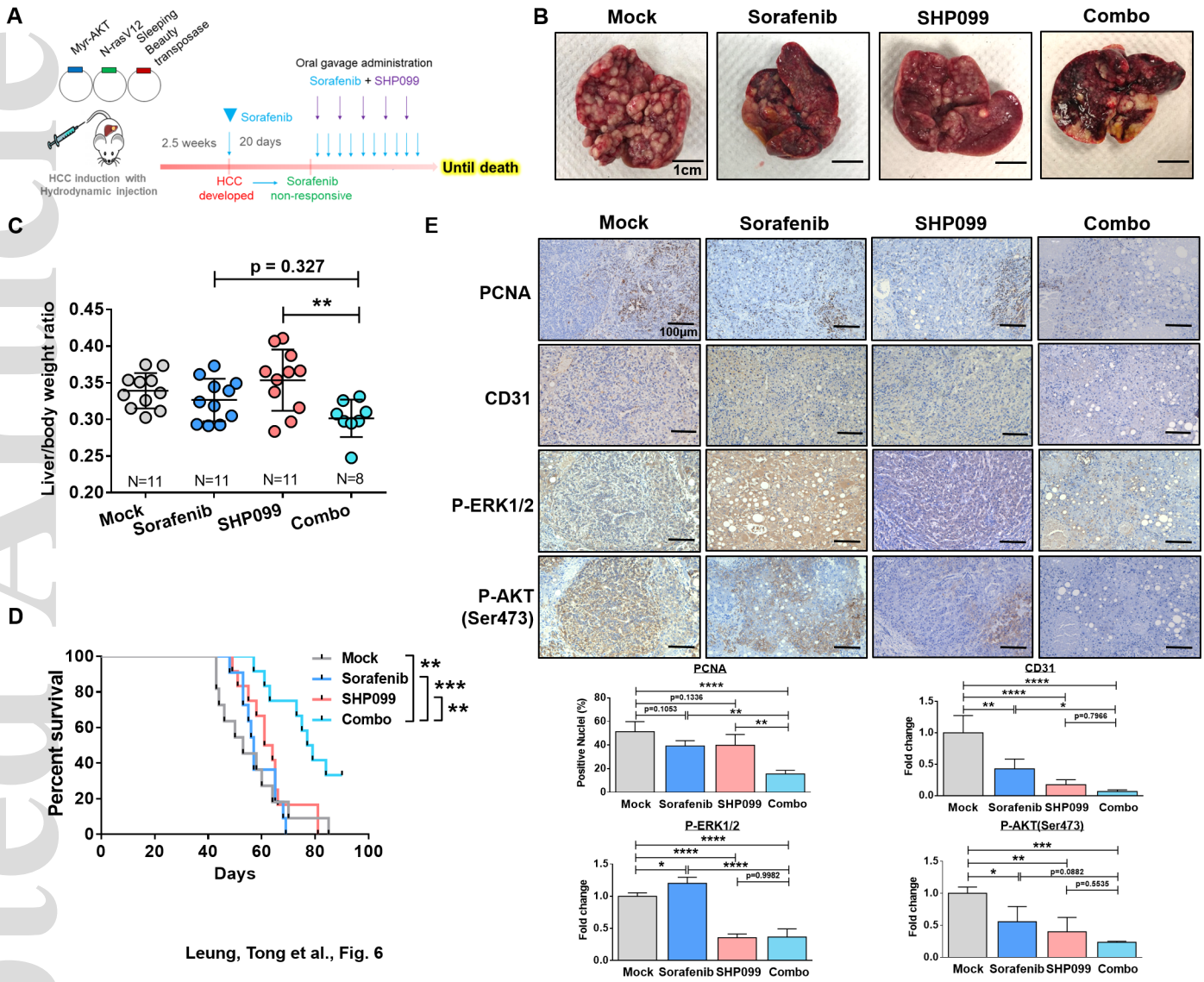

Leung, Tong et al., Fig. 6

hep_30989_f6.tif